Journal of Organometallic Chemistry, 373 (1989) 401–412
Elsevier Sequoia S.A., Lausanne – Printed in The Netherlands
JOM 20055

The syntheses and fluxional properties of mixed halide/methylthio bridged tetramers of trimethylplatinum(IV)

E.W. Abel, K.G. Orrell and D. Stephenson

Department of Chemistry, The University, Exeter EX4 4QD (Great Britain)

(Received April 21st, 1989)

Abstract

Syntheses of the trimethylplatinum(IV) tetramers $[(PtMe_3SMe)_2(PtMe_3X)_2]$ (X = Cl, Br or I) and $[(PtMe_3SMe)_3(PtMe_3Cl)]$ are reported. Both classes of tetramer, by virtue of the two types of bridging ligand, contain two distinct platinum environments. This leads to four different Pt-methyl environments for the structures $[(PtMe_3SMe)_2(PtMe_3X)_2]$ and three such environments for the tetramer $[(PtMe_3SMe)_3(PtMe_3Cl)]$. Variable temperature ^1H NMR studies show that methyl scrambling occurs in each $PtMe_3$ moiety with activation energies ($\Delta G^\ddagger$(298 K)), in the range 61–72 kJ mol^{-1}. $PtMe_3$ groups bonded to two X ligands and one SMe ligand undergo slightly less facile fluxion than those groups attached to one X and two SMe groups. The implications of this fluxionality for symmetrical tetramers (e.g. $[(PtXMe_3)_4]$ are discussed.

Introduction

Trimethylplatinum(IV) derivatives have been known for many decades [1]. An early X-ray diffraction study of trimethylplatinum(IV) chloride [2] showed the compound to be tetrameric with Cl ligands bridging three of four Pt atoms. Later X-ray crystallography on $[(PtMe_3X)_4]$ (X = Br [3], I [4] and OH [5]) revealed analogous cubic tetrameric structures. The methylthio analogue $[(PtMe_3SMe)_4]$ was also shown to be tetrameric both in the vapour phase and in chloroform solution [6], and more recent studies of other thiol compounds $[(PtMe_3SR)_4]$ (R = alkyl, aryl) by NMR and mass spectrometry provide further evidence for tetrameric structures, both in the solid and solution phases [7].

Previous attempts to prepare mixed bridged tetramers such as $[(PtMe_3I)_n(PtMe_3OH)_{4-n}]$ [8,9], $[(PtMe_3SMe)_n(PtMe_3OH)_{4-n}]$ [6], and $[(PtMe_3SMe)_n(PtMe_3SEt)_{4-n}]$ [7] resulted in mixtures from which pure complexes could not be isolated.

We now report on the syntheses of the first acceptably pure samples of mixed bridged platinum(IV) tetramers, namely $[(PtMe_3SMe)_2(PtMe_3X)_2]$ (X = Cl, Br or I)

0022-328X/89/$03.50

Table 1

Analytical data for the complexes $[(PtMe_3SMe)_2(PtMe_3X)_2]$ (X = Cl, Br or I) and $[(PtMe_3SMe)_3(PtMe_3Cl)]$

Complex [a]	Colour	Analysis (Found (calc) (%))	
		C	H
$[(PtMe_3SMe)_2(PtMe_3Cl)_2]$	white	14.4 (14.9)	3.4 (3.7)
$[(PtMe_3SMe)_2(PtMe_3Br)_2]$	white	14.6 (13.9)	2.8 (3.5)
$[(PtMe_3SMe)_3(PtMe_3I)_2]$ [b]	pale yellow	13.3 (12.9)	2.5 (3.2)
$[(PtMe_3SMe)_3(PtMe_3Cl]$	white	15.9 (15.8)	3.1 (4.0)

[a] All complexes decomposed > 200 °C, turning black. [b] Molecular ion of this species identified by mass spectrometry.

and $[PtMe_3SMe)_3(PtMe_3Cl)]$, and on the unexpected fluxionality in these complexes.

Experimental

Preparation of mixed bridged tetramers

To $[(PtMe_3X)_4]$ (0.5 g) was added absolute ethanol (5 cm^3) and excess (3 drops) of tris(methylthio)methane (Aldrich), and the suspension stirred overnight at room temperature. The mixture was then filtered and the solid washed with a small quantity of ethanol and dried. For the halide, X = I, the collected solid was found to be almost exclusively $[(PtMe_3SMe)_2(PtMe_3I)_2]$ with traces of the symmetrical tetramers $[(PtMe_3SMe)_4]$ and $[(PtMe_3I)_4]$. For X = Br, a small amount (< 10%) of $[(PtMe_3SMe)_4]$ was also formed. For X = Cl, the predominant product was $[(PtMe_3SMe)_3(PtMe_3Cl)]$, plus a small amount (< 10%) of $[(PtMe_3SMe)_2(PtMe_3Cl)_2]$.

The complex $[(PtMe_3SMe)_2(PtMe_3Cl)_2]$ was prepared as above but using Ph_3CSMe [10] as the thiolating agent instead of $HC(SMe)_3$.

Analytical data for all four complexes are given in Table 1.

NMR spectra

All NMR spectra were recorded on a Bruker AM250 spectrometer operating at 250.13 MHz (^1H) and 53.53 MHz (^{195}Pt). ^1H shifts are quoted relative to Me_4Si (internal) and ^{195}Pt shifts relative to Ξ (^{195}Pt) 21.4 MHz. A standard variable temperature unit was used to control the NMR probe temperature, values being checked against a Comark digital thermometer and are judged to be accurate to ± 1 °C.

Dynamic information was extracted from the variable temperature ^1H spectra by total bandshape analysis using the authors' adapted version of the original DNMR3 program of Kleier and Binsch [11].

Mass spectra

The molecular ion and fragmentation pattern of $[(PtMe_3SMe)_2(PtMe_3I)_2]$ was obtained using a VG-Micromass MM16F single focussing instrument in this Department.

Results

$[(PtMe_3SMe)_2(PtMe_3X)_2]$ complexes

Static NMR studies. The three halide complexes (X = Cl, Br or I) exhibited similar distinctive NMR features. At temperatures in the range −20 to 30 °C the ^1H spectra display a distinctive seven-line multiplet due to the bridging SMe protons. The intensity distribution in this multiplet is very close to the theoretical ratio 1.0/11.8/49.0/83.6/49.0/11.8/1.0 predicted for Me protons coupling to 0, 1, 2 and 3 ^{195}Pt nuclei [8]. This confirms the tetrameric nature of these complexes. The magnitudes of ^3J(PtSMe) (Table 2) are similar to the value of 15.4 Hz reported for $[(PtMe_3SMe)_4]$ [12]. To lower frequency of the SMe signal are two pairs of PtMe signals with relative intensities 2/1, each with pairs of ^{195}Pt satellites. Examination of the tetrameric structures of these complexes (Fig. 1) shows that two distinct $PtMe_3$ environments are expected, those in the Pt_2X_2 face of the cube being labelled Pt^1Me_3 and those in the $Pt_2(SMe)_2$ face labelled Pt^2Me_3. In a Pt^1Me_3 moiety, two methyls (labelled A) are *trans* to X and one methyl (labelled C) is *trans* to SMe. In a Pt^2Me_3 moiety, one methyl (B) is *trans* to X and two methyls (D) are *trans* to SMe. These four Pt-methyl signals were unambiguously assigned by the following criteria, (i) Their chemical shift and ^2J(PtMe) values were compared with those of the symmetrical tetramers $[(PtMe_3X)_4]$ and $[(PtMe_3SMe)_4]$ (Table 2).

Table 2

^1H NMR shifts [a] and Pt-methyl coupling constants [b] for $[(PtMe_3SMe)_2(PtMe_3X)_2]$

Complex	X	Solvent	T (°C)	δ [c] (Me_A)	δ [d] (Me_B)	δ [e] (Me_C)	δ [f] (Me_D)	δ [g] (Me_E)
$[(PtMe_3SMe)_2$ $(PtMe_3X)_2]$	Cl	$CDCl_3$	−20	1.31	1.30	1.06	1.02	2.34
				(81.6)	(83.8)	(65.1)	(67.6)	(15.8)
	Br	$C_2D_2Cl_4$	20	1.40	1.30	1.16	1.09	2.30
				(81.0)	(82.0)	(66.4)	(67.0)	(15.3)
	I	$C_2D_2Cl_4$	30	1.56	1.35	1.37	1.19	2.29
				(78.5)	(80.0)	(68.0)	(68.0)	(15.7)
$[(PtMe_3X)_4]$ [h]	Cl	$CDCl_3$	−20	1.41	1.41	1.41	1.41	–
				(80)	(80)	(80)	(80)	
	Br	$C_2D_2Cl_4$	20	1.51	1.51	1.51	1.51	–
				(80)	(80)	(80)	(80)	
	I	$C_2D_2Cl_4$	30	1.74	1.74	1.74	1.74	–
				(78)	(78)	(78)	(78)	
$[(PtMe_3SMe)_4]$ [h]	–	$CDCl_3$	30	1.00	1.00	1.00	1.00	2.29
				(71)	(71)	(71)	(71)	(15.3)

[a] In ppm rel. to Me_4Si. [b] ^2J(PtMe) or ^3J(PtSMe) values in Hz in parentheses. [c] *Trans* X, intensity 2. [d] *Trans* X, intensity 1. [e] *Trans* SMe, intensity 1. [f] *Trans* SMe, intensity 2. [g] Bridging S-methyls. [h] Present as low abundance impurities.

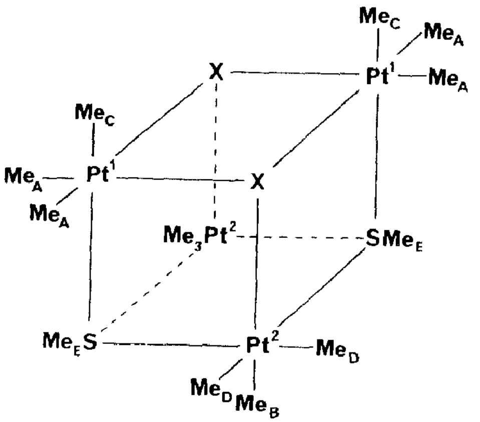

Fig. 1. Structure of the tetramers $[(PtMe_3SMe)_2(PtMe_3X)_2]$ showing the methyl labelling.

Similarities enabled Pt-methyls *trans* X (A, B) and Pt-methyls *trans* SMe (C, D) to be clearly distinguished; (ii) The magnitudes of the ^2J(PtMe) values reflect the different *trans* influences of X and SMe such that for methyls *trans* X the J values are significantly larger than for methyls *trans* SMe [13,14]. In the present complexes the values fall into two distinct groups, namely 65.1–68.0 Hz and 78.5–83.8 Hz. (iii) Variable temperature studies (see later) showed that exchanges occurred between methyls A and C, and between methyls B and D, indicating that these methyl pairs were associated with different $PtMe_3$ moieties.

The full proton NMR data for these complexes are contained in Table 2. Room temperature ^{195}Pt spectra of these three complexes were recorded and the data are listed in Table 3. The two ^{195}Pt signals were assigned by comparison with the shifts reported previously [12] for the symmetrical tetramers $[(PtMe_3X)_4]$ (X = Cl, Br, I or SMe). The data show that bridging halides shield ^{195}Pt nuclei less than bridging SMe groups, causing the Pt^1 nuclei in the Pt_2X_2 face of the cube (Fig. 1) to absorb at higher frequency than the Pt^2 nuclei in the $Pt_2(SMe)_2$ face. Both types of nuclei experience the usual halogen dependence, namely low frequency shifts with increasing atomic number of halogen [15] but the Pt^1 nuclei by virtue of their attachment to two X bridges exhibit a rather greater halogen effect. Very little data exist for scalar Pt–Pt coupling in Pt^{IV} complexes. Our values (Table 3) of ^2J(Pt^{1}Pt^2) are most closely compared with the value of 128 Hz estimated from the ^{13}C NMR spectrum of $[(PtMe_3SMe)_4]$ [12]. Most ^2J(PtPt) values in the literature refer to Pt^{II} systems, where magnitudes are considerably greater than in Pt^{IV} systems and lie in the range

Table 3

^{195}Pt NMR chemical shifts [a] and ^2J(PtPt) coupling constants for $[(PtMe_3SMe)_2(PtMe_3X)_2]$ in $CDCl_3$ at 298 K

X	δ(Pt^1) [b]	δ(Pt^2) [c]	^2J(Pt^{1}Pt^2) (Hz)
Cl	2525	2548	72.0
Br	2372	2436	68.4
I	2004	2222	59.5

[a] Relative to $\Xi(^{195}Pt) = 21.4$ MHz. [b] On X bridged face of cube. [c] On SMe bridged face of cube.

200–970 Hz for bridging S^{2-} or RS^- groups [15]. $^2J(PtPt)$ values involving halogen bridges also depend strongly on the oxidation state of platinum ranging from 125–390 Hz for Pt^{II} to immeasurably small values for Pt^{IV}, e.g. $[(PtXMe_3)_4]$ [12] and $[(PtXMe_3)_2(L\text{–}L')]$ (L–L′ = bridging chalcogen ligand) [16]. The present values of $^2J(Pt^1Pt^2)$ refer to Pt nuclei bridged by one X ligand and one SMe ligand, and it is therefore not unexpected that their magnitudes should be approximate averages of the double SMe-bridged value (128 Hz) and the double X-bridged value (~ 0 Hz).

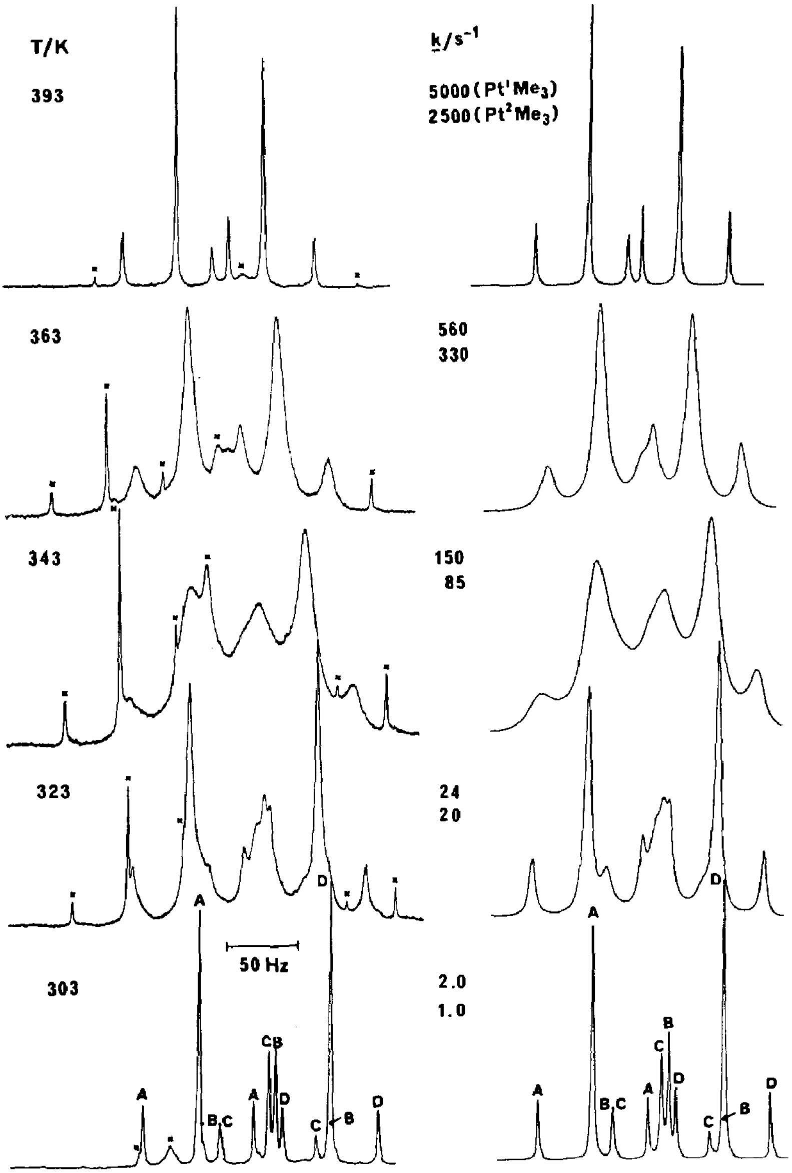

Fig. 2. Variable temperature and computer synthesised ^1H NMR spectra of $[(PtMe_3SMe)_2(PtMe_3I)_2]$ showing the Pt-methyl scrambling. The rate constants refer to Me(C) → Me(A) (Pt^1Me_3), and Me(B) → Me(D), (Pt^2Me_3). The additional signals (×) are due to traces of $[(PtMe_3SMe)_4]$, $[(PtMe_3I)_4]$, and water.

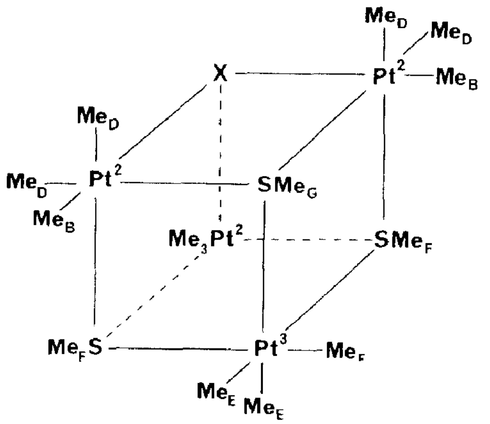

Fig. 3. Structure of the tetramers $[(PtMe_3SMe)_3(PtMe_3X)]$, showing the methyl labelling.

Dynamic NMR studies. When the temperature of the solutions of these complexes was raised from ca. −20 to 100 °C, gross changes occurred in their ^1H spectra. The case of $[(PtMe_3SMe)_2(PtMe_3I)_2]$ is illustrated (Fig. 2). Exchange broadening occurred between the Me_A and Me_C signals, and between the Me_B and Me_D signals. Their bandshapes were accurately recorded in the temperature range ambient to ca. 100 °C and compared with theoretically synthesised bandshapes using the DNMR program. The ^{195}Pt satellite signals were included in the total bandshape fitting procedure and a set of 'best-fit' spectra are shown alongside the experimental spectra in Fig. 2. The additional signals in these spectra are due to traces of $[(PtMe_3I)_4]$, $[(PtMe_3SMe)_4]$ and water, but they did not affect significantly the accuracy of the bandshape analysis. The spectra could be satisfactorily fitted only with two independently varied rate constants, suggesting that the methyl scrambling occurring in the two types of $PtMe_3$ moiety was uncorrelated.

$[(PtMe_3SMe)_3(PtMe_3Cl)]$

The tetrameric structure of this complex is shown in Fig. 3. In this case three trimethylplatinum(IV) moieties, labelled Pt^2Me_3, (in accordance with the $[(PtMe_3SMe)_2(PtMe_3X)_2]$ complexes) contain one methyl (labelled B) *trans* to Cl and two methyls (labelled D) *trans* to SMe. The other trimethylplatinum(IV) moiety, labelled Pt^3Me_3, is unique with its three methyls (E) chemically equivalent and isochronous since they are all *trans* to SMe.

The ^1H and ^{195}Pt data for this complex are given in Table 4 and should be compared with those for the $[(PtMe_3SMe)_2(PtMe_3Cl)_2]$ and $[(PtMe_3SMe)_4]$ com-

Table 4

^1H and ^{195}Pt NMR data for $[(PtMe_3SMe)_3(PtMe_3Cl)]$

δ^a (Pt^2)	δ^b (Me_B)	δ^b (Me_D)	δ^a (Pt^3)	δ^b (Me_E)	δ^c (Me_F)
2544	1.28	1.01	2525	0.95	2.29
(130.6)	(84.3)	(67.5)	(130.6)	(69.3)	(15.2)

[a] Relative to $\Xi(^{195}Pt) = 21.4$ MHz, $^2J(PtPt)$ values in parentheses. [b] Relative to Me_4Si(int), $^2J(PtMe)$ values in parentheses. [c] Relative to Me_4Si(int), $^3J(PtMe)$ value in parenthesis.

Table 5

Magnitudes of ^{195}Pt shifts in trimethylplatinum(IV) chloride/S-methyl tetramers

Complex	δ(Pt) [a] Types of attached bridging ligands			
	3 Cl	2 Cl + 1 SMe	1 Cl + 2 SMe	3 SMe
$[(PtMe_3Cl)_4]$	2479	–	–	–
$[(PtMe_3Cl)_2(PtMe_3SMe)_2]$	–	2525 (Pt^1)	2548 (Pt^2)	–
$[(PtMe_3Cl)(PtMe_3SMe)_3]$	–	–	2544 (Pt^2)	2525 (Pt^3)
$[(PtMe_3SMe)_4]$	–	–	–	2522 [b]

[a] Relative to $\Xi(^{195}Pt) = 21.4$ MHz. [b] Ref. [12]. Converted from shift rel. to $PtCl_6^{2-}$ by +4522 ppm [17].

plexes (Table 2, 3). The ^{1}H shifts and ^2J(PtMe) values for methyls B and D bear a close similarity to the values for the identically labelled Pt-methyls in $[(PtMe_3SMe)_2(PtMe_3Cl)_2]$, while the parameters for methyls E are closely related to those for $[(PtMe_3SMe)_4]$ [12]. The ^{195}Pt shifts for all the chloride complexes $[(PtMe_3Cl)_n(PtMe_3SMe)_{4-n}]$ ($n = 0, 1, 2, 4$) are compared in Table 5, where it will be observed that their variation is very limited (~ 69 ppm) and the magnitudes do not exhibit any simple dependence on the number of attached chloride and/or S-methyl bridging ligands. The shifts follow the order,

$$3\ \mathrm{Cl} < 2\ \mathrm{Cl} + 1\ \mathrm{SMe} \approx 3\ \mathrm{SMe} < 1\ \mathrm{Cl} + 2\ \mathrm{SMe}$$

This trend is not easily rationalised. Assuming ^{195}Pt shifts are dominated by the paramagnetic term σ^{P} of the Ramsey equation, which involves the asymmetry of the 5*d* and 6*p* electronic distributions, the inverse cube of the mean distance of these electrons from the Pt nucleus, and the inverse of the singlet–triplet electronic excitation energy [17], all that can be concluded is that the observed shifts must be the result of more than one term, and probably all three terms, contributing differently for each complex. This is probably a result of the different degrees of strain in the two mixed tetramer cubic geometries.

The other interesting feature of the ^{195}Pt data of $[(PtMe_3SMe)_3(PtMe_3Cl)]$ is the value of $^2J(Pt^2Pt^3)$. Its magnitude (130.6 Hz) is very comparable to that of 128 Hz measured for $[(PtMe_3SMe)_4]$ [12], and strikingly illustrates how scalar spin polarization between Pt nuclei is far more readily transmitted via bridging SMe ligands than via bridging halogens.

Variable temperature ^{1}H NMR studies were carried out in the range −10 to 60 °C to investigate any fluxionality in this complex. At low temperatures three signals (plus ^{195}Pt satellites) due to the Pt-methyls B, D and E were clearly revealed (Fig. 4). On warming the solution, signals due to methyls B & D broadened, coalesced around 30 °C, and subsequently sharpened to a singlet ($\Delta\nu_{1/2} \approx 3$ Hz) at 60 °C. Throughout this temperature rise, the signal due to Pt^3Me_3 (methyls E) remained a sharp singlet, on account of the isochronicity of the three methyls (E). Bandshape analysis of the exchange-broadened signals was performed in the usual way and 'best-fit' spectra computed (Fig. 4).

The tetramer $[(PtMe_3SMe)_2(PtMe_3I)_2]$ was investigated as a possible source of dinuclear Pt^{IV} complexes of type $[(PtMe_3SMe)_2L_2]$ (L = monodentate donor ligands) with the methylthio groups bridging the two platinum atoms. When L was pyridine the iodide face of the mixed tetramer opens up, two moles of $[PtMe_3Ipy_2]$ are formed by cleavage of two Pt–S bonds, leaving the sought-after dinuclear species

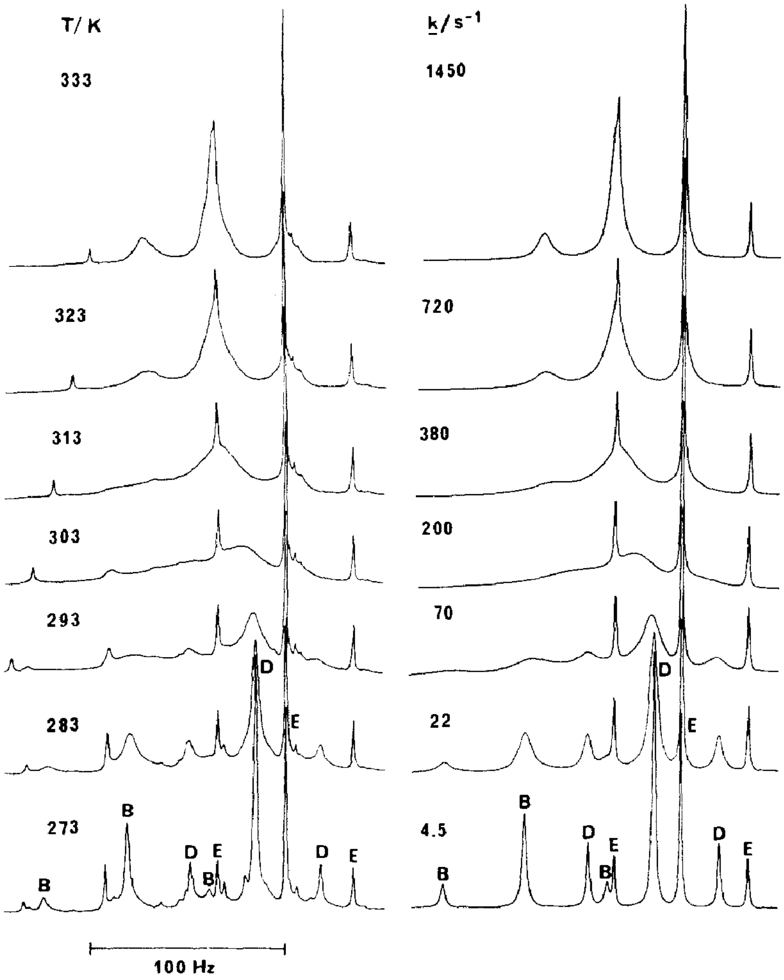

Fig. 4. Variable temperature and computer synthesised ^{1}H NMR spectra of [(PtMe$_3$SMe)$_3$(PtMe$_3$Cl)] showing the Pt-methyl scrambling. The rate constants refer to Me(B) → Me(D) in the Pt^{2}Me$_3$ moieties. Additional weak signals are attributed to traces of [(PtMe$_3$SMe)$_2$(PtMe$_3$Cl)$_2$] and water.

[(PtMe$_3$SMe)$_2$py$_2$], which originally formed the SMe-bridged face of the cubic tetramer. The ^{1}H NMR spectrum of this dinuclear complex was characterised by a 1.0/7.8/17.3/7.8/1.0 quintet at δ1.97 for the methylthio protons, and bands at δ1.22 and 0.44 for platinum methyls *trans* to pyridine and *cis* to pyridine respectively. Only a single set of signals was observed indicating that the pyridines were either exclusively *cis* or exclusively *trans* to each other. An earlier study [18] of the iodide bridged complexes [(PtMe$_3$I)$_2$py$_2$] showed that the *cis* and *trans* bispyridine species could be differentiated by the proton shifts of the Pt-methyl *trans* to pyridine. In the *trans* isomer the ring current of the adjacent pyridine ring shields the methyl protons and produces a shift of δ1.38 compared to δ2.0 for the *cis* isomer. The shift of δ1.22 in the present complex therefore strongly supports the pyridines adopting a mutual *trans* relationship (Fig. 5).

On cooling to ca. $-90\,^\circ$C the spectrum showed no significant changes implying that either inversion of the bridging sulphurs was still rapid at this temperature or that the complex exists in only one invertomeric form. The latter possibility is

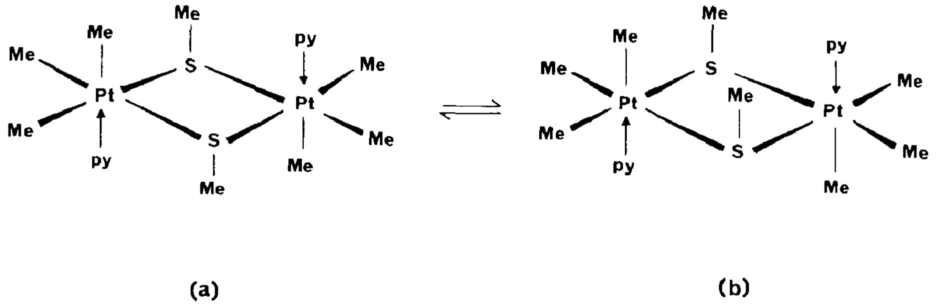
(a) (b)

Fig. 5. Structures of the complexes $[(PtMe_3SMe)_2py_2]$ showing *anti* and *syn* relationships of the bridging S-methyls.

favoured in view of related studies on $[Pt(dppe)(\mu_2\text{-}SMe)_2PtXMe_3]$ (X = Cl, Br, I) [19] where sulphur inversion was not exceptionally fast. However, in these methylthio-bridged complexes there was a strong preference for the invertomers with the bridging S-methyls in an *anti* relationship, and thus it is considered most probable that the present complex $[(PtMe_3SMe)_2py_2]$ exists almost exclusively as the structure (a) in Fig. 5. Above ambient temperatures the pyridine ligands become labile and the tetramer $[(PtMe_3SMe)_4]$ is again formed.

When L was the phosphine PMe_2Ph the SMe-bridged dinuclear complex was formed only as a minor product, the major products being mono-nuclear species. Reaction of the tetramer $[(PtMe_3SMe)_2(PtMe_3I)_2]$ with the bidentate ligand 1,3-diaminopropane yielded a mixture of products which could not be identified.

Discussion

Rate constant data for all four complexes were converted into $\Delta G^{\ddagger}$(298 K) values using standard Eyring rate theory and the results are shown in Table 6. A number of discussion points arise.

Firstly, the energies show a clear halogen dependence with values increasing regularly with increasing halogen mass/size. However, it is somewhat surprising that the Pt^1Me_3 moieties attached to two halogens should show a somewhat weaker

Table 6

$\Delta G^{\ddagger}$ (298 K) [a] (kJ mol^{-1}) values for Pt-methyl scrambling

$[(PtMe_3SMe)_2(PtMe_3X)_2]$		
X	Pt^1Me_3 [b]	Pt^2Me_3 [c]
Cl	65.6	61.3
Br	68.3	66.5
I	71.6	71.5
$[(PtMe_3SMe)_3(PtMe_3X)]$		
	Pt^3Me_3 [d]	Pt^2Me_3 [c]
Cl	?	61.5

[a] Uncertainties ± 0.1 kJ mol^{-1}. [b] 2 Me *trans* X, 1 Me *trans* SMe. [c] 1 Me *trans* X, 2 Me *trans* SMe. [d] 3 Me *trans* SMe.

halogen dependence than the Pt^2Me_3 moieties with only one attached halogen. Previous studies of Pt-methyl scrambling in $[PtXMe_3L]$ and $[(PtXMe_3)_2L]$ (L = coordinated chalcogen ligands) [20] have revealed little halogen dependence, any apparent weak trends being in the opposite direction to the present result.

Secondly, the energy of the Pt-methyl scrambling clearly depends on the nature of the $PtMe_3$ moiety as exemplified by the different values for Pt^1Me_3 and Pt^2Me_3 moieties in $[(PtMe_3SMe)_2(PtMe_3X)_2]$ complexes and the very similar values for Pt^2Me_3 moieties (61.3 and 61.5 kJ mol^{-1}) in both classes of complex (Table 6).

Thirdly, the $\Delta G^\ddagger$ values for all the present complexes fall in the range 61–72 kJ mol^{-1}, which is very comparable to the energy range calculated previously for dinuclear platinum(IV) complexes with bridging halogens, viz. $[(PtXMe_3)_2L]$ (L = open chain ligands such as MeSCHMeSMe [21], MeSCH(SMe)SMe [22], and cyclic ligands $\overline{SCH_2SCH_2SCH_2}$ [23] and $\overline{SCH_2SCH_2SCH_2SCH_2}$ [24]. In contrast, it should be noted that Pt-methyl scrambling in related chelate complexes, $[PtXMe_3L]$ (L = $MeS(CH_2)_2SMe$, $MeS(CH_2)_2SEt$ [25], and $MeSCH_2SCH_2SMe$ [26]) is a less favoured process with $\Delta G^\ddagger$ values in the range 79–100 kJ mol^{-1}. The halogen-bridged dinuclear complexes $[(PtXMe_3)_2L]$ are clearly more closely related to the present Pt^{IV} tetramers so their comparable rates of Pt-methyl scrambling are not unexpected. In the earlier work [21–26], the mechanism of the Pt-methyl scrambling that fully accounted for the DNMR features of the complexes involved 120° rotations of the $PtMe_3$ moiety about its cone axis, this fluxion being thought to be a consequence of the highly non-rigid transition state structures of the ligand switching or pivoting fluxion is $[(PtXMe_3)_2L]$ [21–24] or the ligand 'pancaking' fluxion in $[PtXMe_3L]$ [25,26]. In the present tetramer complexes similar $PtMe_3$ rotations would seem the most likely process, but in this case they cannot be initiated by highly non-rigid 7- or 8-coordinate Pt^{IV} species but by normal octahedral 6-coordinate Pt^{IV} species. If such a process in the present tetramers involved the breaking and re-making of the three ligand bridge bonds, the energy barrier might be predicted to be considerably higher than in complexes where, as a result of internal ligand dynamics, fewer well defined Pt–ligand bonds were involved. The similarity of the scrambling energies in both cases suggests that the fluxion is confined purely to the Pt–methyl bonds. These, however, remain intact throughout the fluxion as evidenced by the ^{195}Pt satellites, but only modest changes in the spatial disposition of the Pt-methyls are required to bring pairs of methyls into identical environments. More precisely, 60° rotations (clockwise or anti-clockwise) of the $PtMe_3$ moieties about their cone axes will produce a transition state structure in which axial/equatorial Pt–methyl distinction is lost. A repeated sequence of these rotations will therefore equate the A and C methyl environments of the Pt^1Me_3 moiety and the B and D environments of Pt^2Me_3. Support for these methyl exchanges being localised in the $PtMe_3$ moieties and not involving the ligand bridge bonds comes from the fact that the fluxions of the two types of $PtMe_3$ group have different activation energies. They are therefore clearly non-concerted, and it is not easy to visualise non-concerted processes which involve cleavage and re-making of Pt–bridge bonds.

The proposed mechanism involving bond angle deformations is clearly somewhat akin to the interconversion of trigonal bipyramidal and square planar configurations of complexes by the Berry twist mechanism [27]. However, the latter process involves appreciably smaller bond angle changes than in the present complexes, which accounts for its much lower activation energy.

The observation of Pt-methyl scrambling in these mixed trimethylplatinum(IV) tetramers clearly implies that this type of fluxion will be present in the symmetrical tetramers $[(PtMe_3Z)_4]$ (Z = halogen, SMe, OH, etc.) [12], where its lack of detection to date is due to the high symmetry of these complexes which renders all the methyl groups isochronous. Thus no internal chemical shift modulation by the fluxion is possible. However, in theory it should be possible to identify any Pt-methyl movement via the long range scalar couplings of methyl carbons of one $PtMe_3$ moiety and the ^{195}Pt nucleus of adjacent $PtMe_3$ moieties, viz. ^3J(CPtZPt) values. In the absence of any Pt-methyl movement, two magnitudes of this coupling would be expected, depending on whether the Pt-methyl carbon is coplanar or at right angles to the face of the cube containing the pair of Pt nuclei. If Pt-methyl scrambling is occurring, a single magnitude of ^3J(CPtZPt) would be observed, which would be a weighted average of the two static values.

An attempt was made to measure such ^3J(CPtZPt) values by recording the ^{13}C spectrum of $[(PtMe_3OH)_4]$ [12]. A spectrum of a $(CD_3)_2CO$ solution of this complex at 50 °C when Pt-methyl scrambling would be expected to be quite rapid revealed ^{195}Pt satellite signals due to the AA′X spin systems (A, A′ = ^{195}Pt, X = ^{13}C) in question [12], but these could not be assigned with any certainty due to limited resolution and low intensities of the signals. However, on cooling the solution to ca. −30 °C these satellite signals broadened appreciably. This could be due to a slowing down of the Pt-methyl scrambling rate, but an equally possible explanation is that it is the result of short spin-lattice relaxation times of the ^{195}Pt nuclei, as a result of strong chemical shielding anisotropy (CSA) contributions, which are dominant at low temperatures [15]. Strong affirmative evidence for Pt-methyl scrambling in symmetrical trimethylplatinum(IV) tetramers $[(PtMe_3Z)_4]$ is therefore still lacking, but the general findings of this present work point to its being highly likely.

References

1 W.J. Pope and S.J. Peachey, J. Chem. Soc., (1909) 571.
2 R.E. Rundle and J.K. Sturdivant, J. Am. Chem. Soc., 69 (1947) 1561.
3 D.E. Clegg and J.R. Hall, J. Organomet. Chem., 22 (1970) 491.
4 G. Donnay, L.B. Coleman, N.G. Krieghoff and D.O. Cowan, Acta Cryst. B, 24 (1968) 157.
5 T.G. Spiro, D.H. Templeton and A. Zalkin, Inorg. Chem., 7 (1968) 2165.
6 J.R. Hall, D.A. Hirons and G.A. Swile, J. Organomet. Chem., 174 (1979) 355.
7 E.W. Abel, K. Kite and B.L. Williams, J. Organomet. Chem., 231 (1982) 271.
8 G.L. Morgan, R.D. Rennick and C.C. Soong, Inorg. Chem., 5 (1966) 372.
9 J.R. Hall and G.A. Swile, J. Organomet. Chem., 44 (1972) 201.
10 W. Seebach, K.-H. Greiss, A.K. Beck, B. Graf and H. Daum, Chem. Ber., 105 (1972) 3280.
11 D.A. Kleier and G. Binsch, DNMR3 program 165, Quantum Chemistry Program Exchange, Indiana University 1970.
12 T.G. Appleton and J.R. Hall, Aust. J. Chem., 33 (1980) 2387.
13 E.W. Abel, A.R. Khan, K. Kite, K.G. Orrell and V. Šik, J. Chem. Soc., Dalton Trans., (1980) 1169.
14 E.W. Abel, A.R. Khan, K. Kite, K.G. Orrell and V. Šik, J. Chem. Soc., Dalton Trans., (1980) 1175.
15 P.S. Pregosin, Ann. Reps. NMR Spectrosc., 17 (1986) 285.
16 E.W. Abel, K.G. Orrell and V. Šik, unpublished work.
17 C.J. Jameson and J. Mason in J. Mason (Ed.), Multinuclear NMR, Plenum Press, New York, 1987, Chapt. 2.
18 J.R. Hall and G.A. Swile, J. Organomet. Chem., 42 (1972) 479.

19 E.W. Abel, N.A. Cooley, K. Kite, K.G. Orrell, V. Šik, M.B. Hursthouse and H.M. Dawes, Polyhedron, 6 (1987) 1261.

20 E.W. Abel, S.K. Bhargava and K.G. Orrell, Prog. Inorg. Chem., 32 (1984) 1.

21 E.W. Abel, A.R. Khan, K. Kite, K.G. Orrell and V. Šik, J. Chem. Soc., Dalton Trans., (1980) 2208.

22 E.W. Abel, T.E. MacKenzie, K.G. Orrell and V. Šik, J. Chem. Soc., Dalton Trans., (1986) 2173.

23 E.W. Abel, M. Booth, G. King, K.G. Orrell, G.M. Pring and V. Šik, J. Chem. Soc., Dalton Trans., (1981) 1846.

24 E.W. Abel, G.D. King, K.G. Orrell, V. Šik, T.S. Cameron and K. Jochem, J. Chem. Soc., Dalton Trans., (1984) 2047.

25 E.W. Abel, I. Moss, K.G. Orrell, V. Šik, D. Stephenson, P.A. Bates, and M.B. Hursthouse, J. Chem. Soc., Dalton Trans., (1988) 521.

26 E.W. Abel, M.Z.A. Chowdhury, K.G. Orrell and V. Šik, J. Organomet. Chem., 258 (1983) 109.

27 R.S. Berry, J. Chem. Phys., 32 (1960) 933.